Asymmetry-symmetry transition of double-sided adhesive tapes

Tetsuo Yamaguchi,[1,*] Hiroyuki Muroo,[2] Yutaka Sumino,[3] and Masao Doi[4]
[1]*Research Center for Advanced Biomechanics, Kyushu University, Fukuoka 819-0395, Japan*
[2]*Institute of Industrial Science, University of Tokyo, Tokyo 153-8505, Japan*
[3]*Faculty of Education, Aichi University of Education, Kariya 448-8542, Japan*
[4]*Toyota Physical and Chemical Research Institute, Nagakute 480-1192, Japan*
(Received 18 April 2012; published 11 June 2012)

We report on the debonding process of a double-sided adhesive tape sandwiched between two glass plates. When the glass plates are separated from each other at a constant rate, a highly asymmetric extension of top and bottom adhesive layers and bending of the inner film are observed first. As the separation proceeds, the elongation of both layers becomes symmetric, and the inner film becomes flat again. When this happens, there appears a local maximum in the force-displacement curve. We explain this asymmetry-symmetry transition and discuss the role of the bimodal force-displacement relation of each adhesive layer. We also discuss the effect of the inner film thickness and the separation rate on the debonding behavior, which causes undesirable early detachment of the double-sided adhesive tape in a certain condition.

DOI: 10.1103/PhysRevE.85.061802 PACS number(s): 82.35.Gh, 68.35.Np, 83.60.Uv, 47.57.Qk

I. INTRODUCTION

Double-sided adhesive tapes are frequently used to fix things, not only as stationary products but also as industrial materials for their wide applicability and adhesion property. Double-sided adhesive tapes have a simple structure: an inner film made of paper, unwoven textile, or plastic film is sandwiched between two pressure-sensitive adhesive layers [1]. Performance of the double-sided adhesive tape depends on various parameters such as the thickness and the rheological properties of the adhesive layer and those of the inner film. In spite of many patents published and commercial products available, few researches have been done on the adhesion property of double-sided adhesive tapes [2].

In contrast, the adhesion property of a single adhesive layer has been studied by many researchers [3]. Various types of mechanical tests such as the peeling test, rolling ball-tack test, and probe-tack test have been used to test the performance of the material [3]. Though they are convenient, the interpretation of such tests is not easy as they involve rather complex deformations [4]. Among these tests, a test which is comparatively amenable to analysis is the probe-tack test in which the two substrates sandwiching the adhesive material are pulled off with their surfaces kept parallel to each other [5].

In the probe-tack test, when the pull-off is started, the debonding stress increases monotonically, reaches a maximum, and then starts to drop abruptly due to nucleation and expansion of cavities [6–19]. At large strains, the debonding stress becomes almost constant ($\sim$0.1 MPa) due to the pressure difference between atmosphere and vacuum for viscoelastic liquids [17,18], while it again increases to have the second peak before the final failure for some viscoelastic solids [20]. It has been pointed out that this bimodal shape of the stress-strain curve is a consequence of the strong adhesion and the elastic hardening of the adhesive materials which form the walls separating the cavities [5].

In this paper, we report on the debonding process of double-sided adhesive tapes in comparison with that of the single adhesive layer. Our aim is to study the relationship between the single adhesive layer and the double-sided adhesive tape, and also to study the effect of the bending elasticity of the inner film on the total debonding behavior.

From the mechanical point of view, the double-sided adhesive tape is a serial connection of two adhesive layers. A naive expectation is that the force-displacement curve of the double-sided adhesive tape is calculable from that of the single adhesive layer by doubling the elongation of the single one. We shall show that this is not the case because the debonding of the double-sided adhesive tape does not take place symmetrically with respect to the inner film: usually one of the adhesive layers is strongly stretched while the other layer is not. In order to have the maximum performance of the double-sided adhesive tape, it is important to avoid such asymmetric debonding behavior. We shall show that the bending deformation of the inner film plays an important role in this respect.

II. EXPERIMENT

A. Sample

The adhesive was prepared by cross-linking acrylic base polymers with isocyanate compounds and the weight ratio of components was the following: butyl acrylate: acrylic acid: 2-hydroxyethyl acrylate: rosin compound: isocyanate compound = 94.9:5:0.1:15:1. The storage modulus G', the loss modulus G'', and $\tan\delta$ of the adhesive were measured with a rheometer (parallel plate, $\phi = 25$ mm, MCR-301, Anton-Paar, Germany). In Fig. 1(a), the corresponding rheological curves are plotted against the reduced frequency. Figure 1(b) schematically shows our double-sided adhesive sample. The thickness of each adhesive layer h_0 was 87.5 μm. For the inner film of the double-sided adhesive tape, we used a black polyethylene terephthalate (PET) film having various thicknesses of $h_{\rm film} = 50, 100, 250$ μm. The bonding between the adhesive layer and the PET film was strong enough that

*yamaguchi@mech.kyushu-u.ac.jp

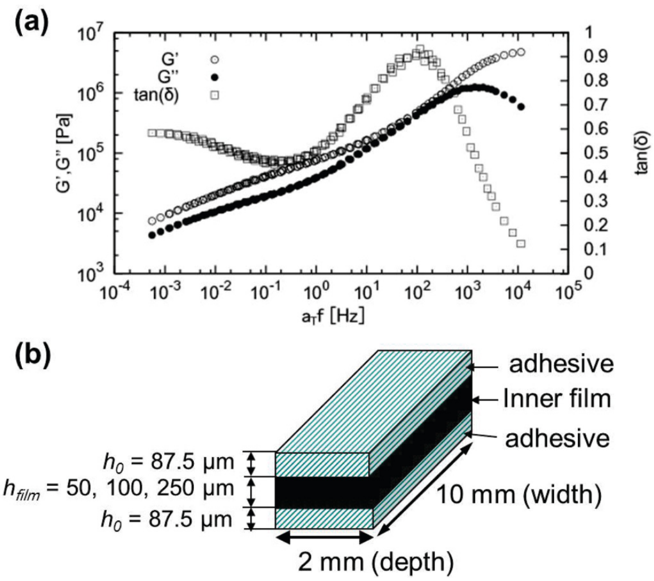

FIG. 1. (Color online) (a) Linear viscoelastic modulus G', G'' (left axis), and $\tan\delta$ (right axis) of the adhesive. The reference temperature is 20 °C. (b) Geometry of a double-sided adhesive tape.

the debonding always took place at the interface between the adhesive layer and the glass plate in our experiments. The adhesive samples were cut to be 10 mm (width) × 2 mm (depth). For quantitative comparisons, a single adhesive layer having the same thickness h_0 and size was also prepared.

B. Apparatus

Figure 2 shows our experimental apparatus. The debonding test was done with the tensile testing machine (type 5564, INSTRON, USA) by sandwiching an adhesive sample between two glass plates. In order to keep the glass surfaces clean, the glass plates (200 × 40 × 5 mm^3) were soaked in a 1 mol/L ethanol solution of sodium hydroxide (NaOH) for 4 h, rinsed

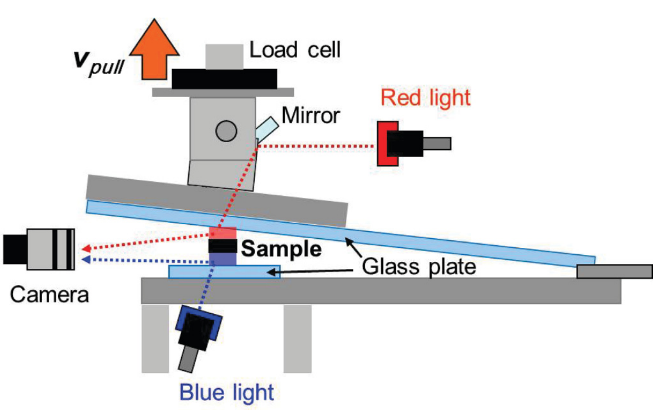

FIG. 2. (Color online) Schematic representation of the experimental apparatus. Observation was performed from the left (perpendicular to the width of an adhesive) by a CCD camera. In order to visualize the top and bottom adhesive layers clearly, the top layer was illuminated by red light and the bottom layer by blue light. Since the distance between the adhesive sample and the right edge of the upper glass plate (≈180 mm) is much larger than the displacement of the machine head (∼3 mm), the two glass plates can be regarded as parallel to each other.

in water twice, kept in bottles filled with distilled water, and dried by whipping nitrogen gas just before testing.

After one side of the protection papers attached on both sides of the adhesive sample was removed, the sample was fixed on the lower glass plate gently with the lowest possible load, and then the other side of the protection paper was removed. After the parallelism between the glass plates was ensured, the upper glass plate was manually brought into contact with the adhesive until the contact force reached about 30 N and the glass plate was kept there for 180 s. The machine head was then driven upward at a constant speed $v_{\rm pull}$, and the pull force was measured by a load cell. Since the distance between the sample and the right edge of the upper glass plate (180 mm) was much larger than the vertical displacement of the machine head (∼3 mm), the two glass plates can be regarded as parallel to each other.

Hereafter, the displacement x stands for the displacement of the machine head. It is important to note that due to the finite compliance of our experimental apparatus, the machine displacement is not the same as that of the top glass plate relative to the bottom, i.e., the change of the distance between the plates [21,22]. The effects of the finite compliance will be discussed later. The origin of the displacement was set at the position where the measured force changed its sign (i.e., from compressive to tensile force).

Experiments were conducted at three pull velocities, $v_{\rm pull} =$ 10, 100, and 1000 μm/s for the double-sided adhesives. For quantitative comparisons, experiments using a single adhesive layer were also done at 5, 50, and 500 μm/s so that the nominal strain rate $v_{\rm pull}/h_0$ becomes the same as that for the double-sided adhesive tape.

In order to visualize the top and the bottom adhesive layer clearly, the top adhesive layer was illuminated by red light from the top and the bottom by blue light from the bottom. This also allowed us to identify the position of the inner film clearly as the boundary of the two colored regions since the black PET film does not transmit light. Debonding images were taken by a CCD camera (KEYENECE,VHX-200, Japan) from the direction vertical to the long axis (width) of the sample. All experiments were conducted at room temperature.

III. RESULTS AND DISCUSSION

A. Force-displacement curves of a single adhesive layer

Figure 3 shows the force-displacement curves of a single adhesive layer for three different pull velocities. It is seen that in all cases the force first exhibited a distinct peak, then increased gradually, and finally fell to zero. This behavior is similar to that observed in the probe-tack test of soft viscoelastic solid adhesives [5,9], and the mechanism is considered to be the same: the first peak of the force corresponds to the nucleation and expansion of cavities to relax the negative pressure inside the adhesive layer [12,13,17,18], and the following gradual increase of the force corresponds to the elongation of the walls between cavities. The final falling of the force corresponds to the detachment of the adhesive layer from the glass plate.

We also measured the force-displacement curve of the machine itself by crumping the upper and lower glass plates firmly without adhesives. This is indicated by the curve denoted as

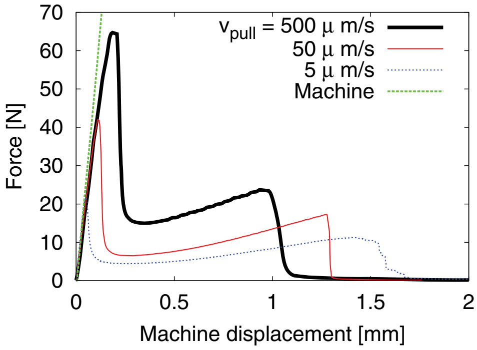

FIG. 3. (Color online) Force-displacement curves of a single adhesive layer at three different pull velocities v_{pull}. Force-displacement curve for the machine itself was also measured by crumpling firmly the upper and lower glass plates.

"Machine" in Fig. 3. The slope of this curve gives the machine spring constant k_{machine}, which was 5.3×10^5 N/m. The initial slope of the curve including the adhesive layer is given by $k_{\mathrm{meas}} = (1/k_{\mathrm{adh}} + 1/k_{\mathrm{machine}})^{-1}$. From this, we obtained the spring constant of the adhesive layer as $k_{\mathrm{adh}} = 2 \times 10^6$ N/m, which is about 4 times larger than that of the machine. Therefore the initial slope of the measured force-displacement curve is dominated by the compliance of the machine [21,22]. On the other hand, the effect of the machine compliance becomes negligible for large displacement ($x > 0.3$ mm) since the displacement caused by the machine compliance is at most 20 N/$k_{\mathrm{meas}} \approx 0.04$ mm.

The initial spring constant of the adhesive layer can be estimated theoretically by taking into account the confinement [5]. If a strip of thin elastic layer with the edge lengths d_0 (depth) and w_0 (width) having thickness h_0 ($h_0 \ll d_0 \ll w_0$) and shear modulus μ is attached to two rigid substrates on both top and bottom surfaces, the effective Young's modulus of the adhesive layer for the change of the gap distance between the substrates is given by $E_{\mathrm{eff}} \sim \mu(d_0/h_0)^2$ [13,14]. The initial spring constant of the layer is therefore given by $k_{\mathrm{adh}} = E_{\mathrm{eff}} d_0 w_0/h_0$. In the present experiment, $\mu \sim 1 \times 10^5$ Pa, $d_0 \sim 1 \times 10^{-3}$ m, $w_0 \sim 1 \times 10^{-2}$ m, and $h_0 \sim 1 \times 10^{-4}$ m. Therefore k_{adh} is estimated to be 10^6 N/m, which is comparable to the measured value.

The force-displacement curve depends only weakly on the pull velocity. With the increase of the pull velocity, the maximum force increased slightly (approximately in a logarithmic manner) and the maximum displacement decreased slightly, but the overall shape of the force-displacement curve was the same for all pull velocities we measured.

B. Force-displacement curve of a double-sided adhesive tape

Figure 4(a) shows a typical force-displacement curve of a double-sided adhesive tape. The thickness of the inner film h_{film} is 100 μm and the pull velocity v_{pull} is 100 μm/s. Figure 4(b) shows the corresponding snapshots of the side view. The inner film is seen at the boundary between the red-colored region (top adhesive layer) and the blue-colored region (bottom adhesive layer). The observation was not possible for displacement $x < 0.2$ mm since the gap between two glass plates was too small to see. In the range $x > 0.2$ mm, the asymmetric fibrillation already started, as shown in Fig. 4(b) (i) and (ii). In some part, the top side of the adhesive layer was strongly elongated and fibrils were seen, while the bottom side was not elongated. In another part, the bottom side was elongated and the top side was not. Accordingly, the inner film was bent and thus the deformation of the adhesive layer was separated into two domains, elongated or nonelongated regions existing both in top and bottom layers complementarily.

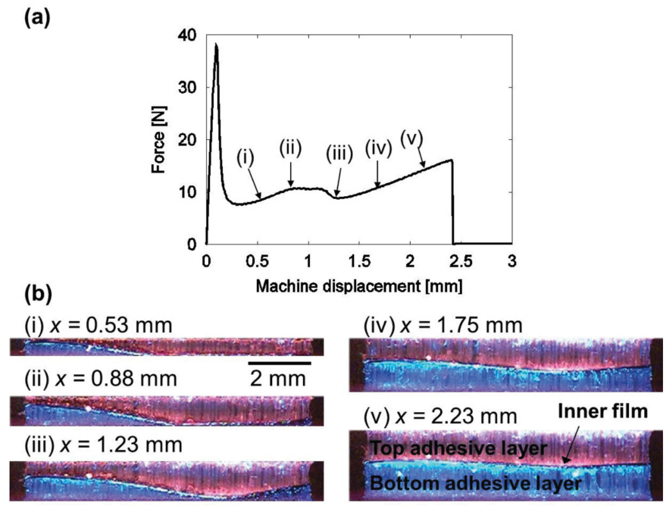

FIG. 4. (Color online) (a) Typical force-displacement curve for a double-sided adhesive tape: $h_{\mathrm{film}} = 100$ μm and pull velocity $v_{\mathrm{pull}} = 100$ μm/s. Second peak appeared at $x \approx 1$ mm. (b) Snapshots for various displacement values corresponding to the letters in (a). At the boundary between two colors, the inner film is located.

As the displacement increased, the nonelongated side started to be elongated. As the elongation of this side took place faster than the other side, the symmetry was gradually recovered [see Fig. 4(b) (iv)]. Eventually, the inner film became almost flat [Fig. 4(b) (v)] before the detachment from one side of the glass plates occurred.

Corresponding to the transition from the asymmetric deformation to the symmetric deformation of the inner film, the force-displacement curve exhibits a characteristic feature which is not observed for a single adhesive layer, i.e., the second peak appears around $x = 1$ mm. If the deformation of adhesive layers keeps symmetry during the debonding process, the force-displacement curve has almost the same shape as that of a single adhesive layer. The second peak is therefore the result of the asymmetry-symmetry transition.

Figures 5(a) and 5(b) show the force-displacement curves of double-sided adhesive tapes having various inner film thicknesses. The pull velocities v_{pull} are 10 and 100 μm/s, respectively. Though there are some variations among these curves, the same characteristics are seen: the second peak appears around $x \sim 1$ mm and the detachment of the adhesive takes place at about $x \sim 2.5$ mm.

C. Simple model

To the first approximation, the asymmetry-symmetry transition can be understood by a simple model. Let us regard the double-sided adhesive tape as a serial connection of two

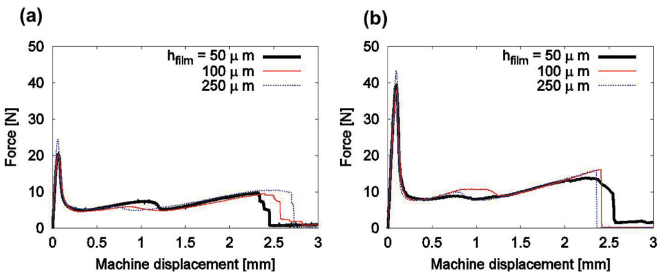

FIG. 5. (Color online) Force-displacement curves at (a) $v_{\text{pull}} = 10\ \mu$m/s and (b) $v_{\text{pull}} = 100\ \mu$m/s for various double-sided adhesive tapes having different thicknesses of the inner film.

nonlinear springs whose mechanical property is described by the nonlinear force-displacement curve $f(d)$ shown in Fig. 6(a) [note that $f(d)$ is the force-displacement curve of an adhesive itself and different from those in Fig. 3 including the machine compliance effect].

Consider the situation that the distance between the glass plates is changed by x'. (x' is different from the machine displacement x, as discussed in the previous sections due to the deformation of the machine, but the difference is negligible for $x > 0.3$ mm.) Let d be the displacement of the inner film. Then the change of the thickness of the bottom layer and that of the top layer are d and $x' - d$, respectively. For a given value of x', d is determined by the balance of the restoring force of the two layers:

$$f(d) = f(x' - d) \tag{1}$$

The graphical solutions for this equation are shown in Fig. 6. For very small d, there is only one solution. However, such deformation is not seen as it corresponds to very small values of x ($x < 0.2$ mm).

With the increase of x', there appear three solutions as shown in Fig. 6(a). The outer two solutions (indicated by filled circles) correspond to the asymmetric deformation of the layer ($d \neq x'/2$), while the central solution corresponds to the symmetric deformation ($d = x'/2$). Notice that in the case of Fig. 6(a), the symmetric solution is unstable since $df(x)/dx$ is negative there. To see this, suppose that the inner film moves upward slightly from the equilibrium point, then the restoring force from the bottom layer decreases while the restoring force from the top layer increases. Therefore, the inner film moves further upward. On the other hand, at the asymmetric solution in Fig. 6(a), $df(x)/dx$ is positive and the solution is stable.

With further increase of x', we have the situation shown in Fig. 6(b). In this case, the outer solutions become unstable, and the central solution becomes stable. Therefore, with the increase of the displacement of the top plate, the deformation of the double-sided tapes transforms from the symmetric (for the invisibly small deformation) to the asymmetric and then to the symmetric again. The observed behavior of the asymmetric to symmetric transformation is thus explained by this simple model.

Figure 6(c) shows three curves for quantitative comparisons. The first one is the force-displacement curve of the single adhesive layer at $v_{\text{pull}} = 50\ \mu$m/s, The second is the force-displacement curve of the double-sided adhesives at $v_{\text{pull}} = 100\ \mu$m/s [same as that in Fig. 4(a)]. The third is the curve drawn under the assumption of symmetric elongation of both adhesive layers in the following way. The displacement $x_{\text{symmetric}}$ is estimated by

$$\begin{aligned} x_{\text{symmetric}} &= 2[x_{\text{single}} - f(x_{\text{single}})/k_{\text{machine}}] + f(x_{\text{single}})/k_{\text{machine}} \\ &= 2x_{\text{single}} - f(x_{\text{single}})/k_{\text{machine}}, \end{aligned} \tag{2}$$

where $f(x_{\text{single}})$ is the force-displacement curve of the single adhesive layer at $v_{\text{pull}} = 50\ \mu$m/s shown in Fig. 3. In this calculation, acceleration of the top glass plate just after the first force peak is neglected and the deformation of each adhesive layer at a constant rate is assumed throughout the debonding process.

It is clearly seen that the force-displacement curve for the double-sided adhesive tape is in good agreement with that for the single adhesive layer at $x < 1$ mm, which corresponds to the situation where only one side of the double-sided adhesive is elongated, while it fits well with the curve drawn by assuming the symmetric deformation of both layers at $x > 1$ mm. This force-displacement behavior again supports the observed asymmetry-symmetry transition.

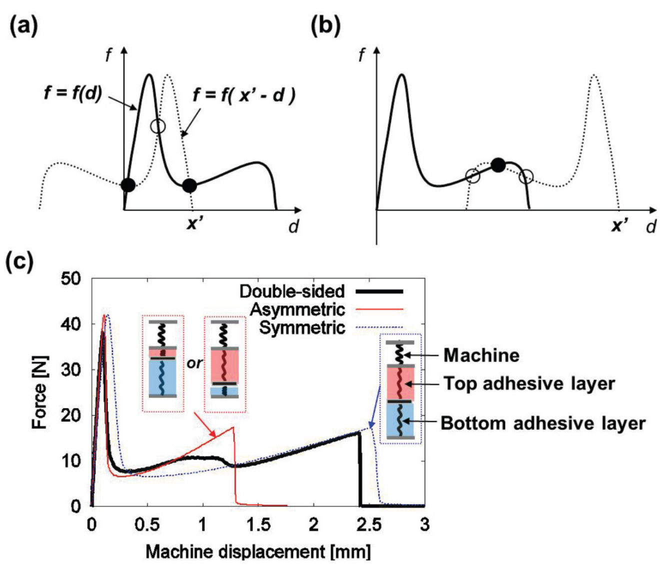

FIG. 6. (Color online) (a), (b) Graphical solutions for the displacement of the inner film d for a given gap between the upper and lower glass plates x'. (a) At a small gap, two stable asymmetric solutions (indicated by filled circles) and one unstable symmetric solution (open circle) are found as the intersections between two curves $f = f(d)$ and $f = f(x' - d)$. (b) At a large gap, one stable symmetric solution and two unstable asymmetric solutions are found. Note that the difference between x' and x (displacement of the machine) is negligible in both cases ($x > 0.3$ mm). (c) Quantitative comparisons of three different force-displacement curves. "Double-sided" is the force-displacement curve of the double-sided adhesive at $v_{\text{pull}} = 100\ \mu$m/s [same as that in Fig. 4(a)], "Asymmetric" is the force-displacement curve of the single adhesive layer at $v_{\text{pull}} = 50\ \mu$m/s, and "Symmetric" is the curve drawn under the assumption of symmetric elongations of both adhesive layers whose displacement is determined by Eq. (2).

D. Early detachment

Figure 7(a) shows the force-displacement curves at a larger pull velocity $v_{\text{pull}} = 1000\ \mu$m/s. For the samples with thin

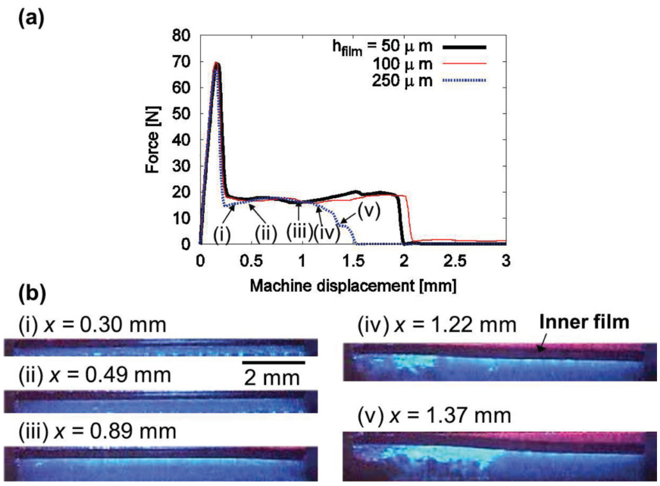

FIG. 7. (Color online) (a) Force-displacement curves at pull velocity 1000 μm/s for double-sided adhesive tapes with various thicknesses of the inner film. Early detachment occurred for the sample of $h_{\rm film} = 250\ \mu$m. (b) Snapshots for the sample of $h_{\rm film} = 250\ \mu$m at various displacement values corresponding to the letters in (a).

and intermediate inner films ($h_{\rm film} = 50$ and 100 μm), the second peaks are still seen and the elongation continues until $x \sim 2$ mm. On the other hand, for the sample having a thick inner film $h_{\rm film} = 250\ \mu$m, the second peak is not so clear and the adhesive tape fails at the smaller displacement of $x \sim 1.5$ mm.

When this early detachment is observed, the asymmetry-symmetry transition fails to take place: the elongation of the adhesive layer takes place only at one side of the tape. Actually, as shown in Fig. 7(b), only the bottom adhesive layer is elongated and ruptures without having elongation of the top layer.

Figure 8 summarizes the adhesive performance of the double-sided adhesive tapes in various inner film thickness and pull velocity conditions. In Fig. 8(a), we plotted the adhesion energy, which is defined by the work needed to fully debond an adhesive tape (i.e., area of the force-displacement curve) divided by the sample area (10 mm $\times$ 2 mm $= 2 \times 10^{-5}$ m^2). The average and the standard deviation were obtained from five trials. For quantitative comparisons, the adhesion energy for a single adhesive layer was also plotted at the same nominal strain rate (pull velocity/adhesive thickness) as the double-sided adhesive tape. It is seen that the adhesion energy of all samples increased with the pull velocity, and the values for the double-sided adhesive tapes were larger than that of the single adhesive layer. On the other hand, a large deviation was found for $h_{\rm film} = 250\ \mu$m and $v_{\rm pull} = 1000\ \mu$m/s. Figure 8(b) shows the normalized adhesion energy, defined by the ratio of the adhesion energy between a double-sided tape and a single adhesive layer. If the deformation is symmetric, it is expected to take a value of 2; in our experiments, the normalized adhesion energy was 1.5–1.7 in most cases, while it was significantly small again for $h_{\rm film} = 250\ \mu$m and $v_{\rm pull} = 1000\ \mu$m/s.

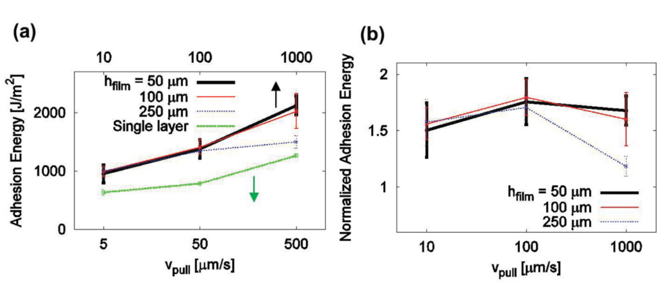

FIG. 8. (Color online) (a) Relationship between the pull velocity (top axis) and the adhesion energy for double-sided adhesive tapes. For quantitative comparisons, the adhesion energy for a single adhesive layer was also plotted against the pull velocity (bottom axis) at the same nominal strain rate as the double-sided adhesive tape. (b) Relationship between the pull velocity and the normalized adhesion energy for the double-sided adhesive tapes.

We now discuss the reasons why such early detachment occurs for thick inner film and at large pull velocity. In the discussion given in Sec. III C, the inner film is assumed to remain parallel to the glass plate throughout the debonding process. In reality, the displacement of the inner film depends on the horizontal position, and therefore the inner film must be bent. The bending deformation of the inner film and resulting in-plane tension (due to its inextensibility) create the lateral coupling of the adhesive layers.

Consider the situation that the displacement x is small so that the asymmetric deformation is stable [the situation shown in Fig. 6(a)]. In such a situation, the elongation of the top and bottom layers alternates as shown in Fig. 9(a), where the top layer is elongated at the left, not elongated in the middle, and is elongated again at the right. At the boundary between such asymmetric domains, there exists a symmetric region where both adhesive layers are elongated and the inner film is bent, creating the boundary energy between the asymmetric domains. Such a multiple domain state is not the state of

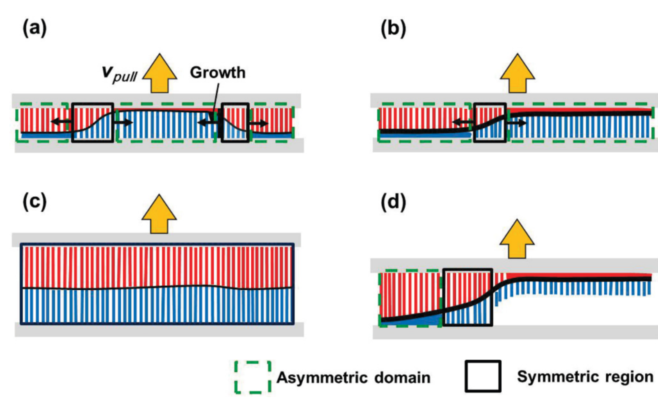

FIG. 9. (Color online) Illustrations of two different cases: (a) thin inner film case and (b) thick inner film case. If the inner film is thin (a), the double-sided adhesive tape forms several small asymmetric domains and symmetric regions. When the machine head is displaced further to reach the state where the symmetric elongation is stable, the symmetric regions start to grow and coalesce easily with each other, resulting in the formation of the symmetric monodomain (c). On the other hand, if the inner film is thick (b), few and large asymmetric domains appear and it takes much longer time for the symmetric regions to coalesce with each other. In particular, if the pull velocity is large, detachment of the elongated side tends to occur before the system reaches the symmetric state (d).

energy minimum but it is a metastable state. Therefore the number of asymmetric domains (or the number of boundaries) does not change as long as the asymmetric deformation is stable. On the other hand, when the displacement x is increased further, the asymmetric deformation becomes unstable, and the system turns into the symmetric monodomain state, as shown in Fig. 9(c). This will take place by the growth of the symmetric regions (i.e., the boundaries between the asymmetric regions). As these symmetric regions grow, the neighboring domains merge and coalesce to form the symmetric monodomain.

The time for such coalescence depends on the size of the asymmetric domains. The larger the domain is, the longer the coalescence time is. If the inner film is thin [as in Fig. 9(a)], the energy cost for sigmoidal deformation is not so large that the system is separated into several asymmetric domains. In such a case, the asymmetric domains become small and the symmetric boundary regions are able to coalesce with each other easily, leading to the symmetric monodomain state as shown in Fig. 9(c). On the other hand, if the inner film is thick [as in t Fig. 9(b)], large and few asymmetric domains appear. In this case, it takes much longer for the symmetric regions to coalesce with each other. In particular, if the pull velocity is large, detachment of the elongated side tends to occur before the system reaches the symmetric state, as illustrated in Fig. 9(d). The above scenario is rather qualitative. Numerical simulations are being conducted and the results will be reported in a separate paper.

IV. CONCLUSION

We have observed the asymmetry to symmetry transition in the debonding of double-sided adhesive tapes and have shown that this is due to the bimodal force-displacement curves of two adhesive layers and the bending of the inner film. We have shown that the asymmetry to symmetry transition is important in the performance of double-sided adhesive tapes: failure of the transition leads to early detachment of the tape from the glass plate. We have experimentally shown that the failure can occur when the inner film is thick and the separation velocity is large, and have given a simple picture to explain the behavior. Despite the findings of this study, several efforts remain to be made. For example, theoretical or numerical studies are necessary for further understanding of the underlying mechanisms, and more systematic experiments using adhesive layers showing various force-displacement relations are worth trying. These will be reported elsewhere in the near future.

ACKNOWLEDGMENTS

The authors thank T. Okuzono for helpful comments. Y.S. is supported by the JSPS (Grant No. 21-3566) Research Fellowships for Young Scientists from the MEXT of Japan. This work is also supported by a Grant-in-Aid for Scientific Research (20244067) from the Ministry of Education, Culture, Sports, Science and Technology of Japan.

[1] D. Satas, *Handbook of Pressure Sensitive Adhesive Technology*, 2nd. ed., Vol. 1 (Van Nostrand Reinhold, New York, 1989).
[2] T. Tsukatani, Y. Hatano, and H. Mizumachi, J. Adhesion Soc. Japan **28**, 353 (1992).
[3] A. V. Pocius, *Adhesion and Adhesives Technology* (Hanser, Munich, 1996).
[4] C. Gay and L. Leibler, Phys. Today **52**, 48 (1999).
[5] K. R. Shull and C. Creton, J. Polym. Sci. B **42**, 4023 (2004).
[6] A. Zosel, Colloid Polym. Sci. **263**, 541 (1985).
[7] A. Zosel, J. Adhesion **30**, 135 (1989).
[8] A. Zosel, J. Adhesion **34**, 201 (1991).
[9] H. Lakrout, P. Sergot, and C. Creton, J. Adhesion **69**, 307 (1999).
[10] C. Creton and H. Lakrout, J. Polym. Sci. B **38**, 965 (2000).
[11] T. Yamaguchi, K. Koike, and M. Doi, Europhys. Lett. **77**, 64002 (2007).
[12] T. Yamaguchi, H. Morita, and M. Doi, Eur. Phys. J. E **20**, 7 (2006).
[13] T. Yamaguchi and M. Doi, Eur. Phys. J. E **21**, 331 (2006).
[14] M. Doi and T. Yamaguchi, J. Non-Newtonian Fluid Mech. **145**, 52 (2007).
[15] K. Brown, J. C. Hooker, and C. Creton, Macromol. Mater. Eng. **287**, 163 (2002).
[16] K. R. Brown and C. Creton, Eur. Phys. J. E **9**, 35 (2002).
[17] S. Poivet, F. Nallet, C. Gay, and P. Fabre, Europhys. Lett. **62**, 244 (2003).
[18] S. Poivet, F. Nallet, C. Gay, J. Teisseire, and P. Fabre, Eur. Phys. J. E **15**, 97 (2004).
[19] J. Teisseire, F. Nallet, P. Fabre, and C. Gay, J. Adhesion **83**, 613 (2007).
[20] C. Creton, J. Hooker, and K. R. Shull, Langmuir **17**, 4948 (2001).
[21] B. A. Francis and R. G. Horn, J. Appl. Phys. **89**, 4167 (2001).
[22] D. Derks, A. Lindner, C. Creton, and D. Bonn, J. Appl. Phys. **93**, 1557 (2003).